

Room Temperature Mechanical Thinning and Imprinting of Solid Films

Graham L. W. Cross,* Barry S. O'Connell, H. Özgür Özer, and John B. Pethica

SFI Trinity Nanoscience Laboratory, Department of Physics, Trinity College, Dublin 2, Ireland

Received October 19, 2006; Revised Manuscript Received December 11, 2006

ABSTRACT

The mechanical patterning of thin films has received recent attention due to significant potential for efficient nanostructure fabrication. For solid films, mechanically thinning wide areas remains particularly challenging. In this work, we introduce a new plastic ratchet mechanism involving small amplitude (<10 nm), oscillatory shear motion of the forging die. This isothermal mechanism significantly extends mass transport across surfaces, broadening the scope of nanoscale processing for a potentially wide class of solid ductile materials.

The mechanical resilience of thin films and coatings is a matter of considerable concern in many technologies, where scratching, cutting, and indenting type contact geometries can lead to deformation and wear of these surfaces. The converse problem of how to pattern thin films by mechanical means has recently come of interest in the context of nanostructure fabrication, with various current forms including hot embossing,¹ cutting,² solid forging,³ and rigid⁴ and soft molding⁵ and applications including inorganic semiconductor lithography, organic electronics,⁶ diffractive optics,² and bioengineering.⁷ In room temperature forging where a solid film is thinned by mechanical imprint stress alone, the impression formed in the film is the residual shape left by plastic (inelastic) squeeze flow under the die, plus any relaxations during unloading. Accurate shape fidelity requires a means of efficient mass transport across a wide range of possible die widths. Ideally, the squeezed film should become arbitrarily thin, but in practice a finite thickness is reached for a given width. This residual layer thickness is caused by die friction and inherent shear strength of the film⁸ and also by constraint pressure from the material extruded at the edge of the squeeze zone.⁹ Increasing the applied normal forming pressure to try to further thin the layer tends instead to produce elastic distortions of the die and degrades shape fidelity.^{8,10}

Inelastic straining of a material at a temperature T can be pictured as a rate activated process in the Eyring description¹¹

$$\dot{\epsilon} = \dot{\epsilon}_0 e^{-(E_a - \sigma V)/k_B T}$$

where $\dot{\epsilon}$ is the strain rate, σ the applied mechanical stress, and E_a and V are the activation energy and volume for the

specific deformation process considered. Inelastic flow in conventional imprinting employing a simple, monotonic loading stroke can be improved either by material choice to reduce E_a or simply by increasing T , but each has its downside; raising the temperature to speed the flow, for example, means the system must be cooled before unloading, which gives differential compressive stresses, shape relaxations, and problems of adhesion.¹² In contrast, influencing the stress-volume energy term of Eyring's expression has been unexplored for the planar geometry—mechanical stress is applied as normal loading, which generates considerable parasitic hydrostatic pressure in addition to the deviatoric stress that activates plastic flow. We now show that modifying the stress σ by applying small amplitude oscillatory shear, at only moderate normal loads, cumulatively provides considerable improvements in squeeze flow and significantly improves shape fidelity and control for nanoforming, at both mesoscopic and nanometer scales.

Small amplitude oscillatory shear forming (SAOSF) for a simple die shape is summarized in panels a–d of Figure 1. (The term small amplitude used here is with reference to forming fidelity, where the magnitude of motion is small with respect to the size of the die shapes. It does not imply a linear constitutive response of the formed material.)

A flat punch of hard, stiff material and a supported, softer film are brought into contact (a) and a normal load is applied (b). Inelastic displacement of material due to this normal loading ceases if edge constraints or elastic distortions are built up in elastoplastic solid forging⁸ or material relaxation time scales are not allowed for in the case of liquid molding.¹³ Once the contact is established, a small oscillatory motion is applied in the plane of the soft film (Figure 1c), shearing it and driving further inelastic flow. Die removal completes the process to leave a thinned film as shown (Figure 1d).

* Corresponding author. Graham.Cross@tcd.ie.

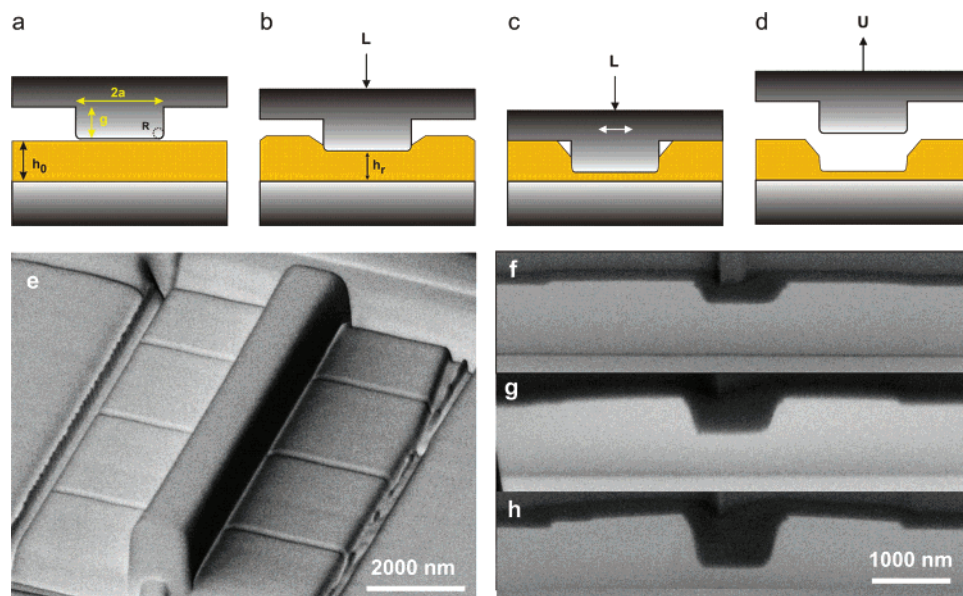


Figure 1. Principle and operation of small amplitude oscillatory shear forming (SAOSF). (a) A rigid punch is to form a ductile, thin solid film (yellow) by establishing direct mechanical contact (b). Plastic strains are generated by augmenting the normal contact load with a small oscillatory motion in the plane of the film (c). After sufficient cycles, die and film are separated leaving the thinned film (d). A demonstration of the effect is provided for the single tooth, plane strain stamp (e), where a normal pressure of 50 MPa (f) leads to only minor extrusion of a solid polystyrene film (FIB cross-section micrograph). The addition of 10 nm (g) and 20 nm (h) amplitude oscillatory shear motion (along an axis in-plane to the image, parallel to the film, and orthogonal to the long axis of the stamp) produces the pronounced forming enhancement shown.

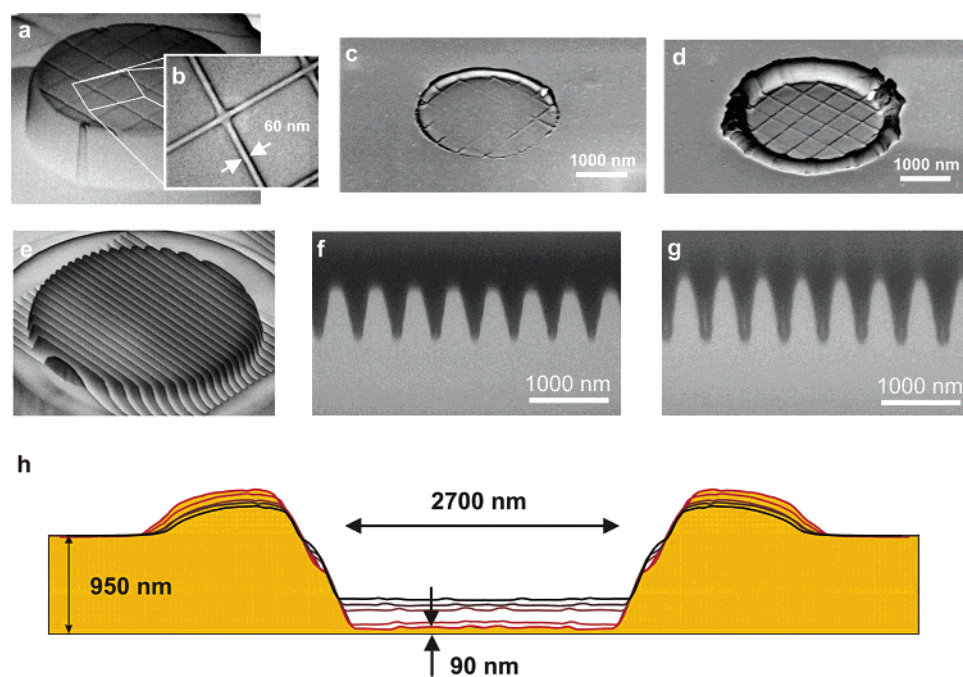


Figure 2. Resolution, parallelism, and high aspect ratio mass transport performance of SAOSF. The 60 nm lines (b) decorating a cylindrical flat punch (a, 3000 nm punch diameter) are barely visible under the 90 MPa normal load of (c) but are well reproduced after extensive shear forming into a glassy polystyrene film (d). In (g), filling into cavities between parallel, 500 nm pitch line patterns on the die of (e) is enhanced over normal loading (f). Significant long-range surface mass transport in solid polymer is shown in (h) by the incremental residual layer thinning by SAOSF from an aspect ratio of 7 (black AFM scan profile—no shear) to 30 (red profile—30 nm shear amplitude) show no loss in thickness uniformity (here, the stamp of (a) was used).

We have experimentally characterized SAOSF using simple die shapes mounted in a nanoindentation system,^{8,14} which provides control of applied load and measurement of resulting displacement of the die in the direction normal to the film plane. This normal displacement provides a measure

of extrusion, residual film thickness, and mass transport during imprint. Shear was added via a monolithic shear piezo element on which the sample was mounted; the shear motions of the die with respect to sample were monitored continuously during imprint by a differential laser vibrometer with

sub-nanometer resolution. The die of Figure 1e was used to give plane strain of a 950 nm thick solid polystyrene film, at room temperature. While 50 MPa normal pressure alone produces little extrusion (Figure 1f), the additional application of a 10 and then a 20 nm amplitude shear oscillation results in significantly increased net material flow while replicating the die shape, as shown in panels g and h of Figure 1. That is, added shear amplitudes of 1 and 2% of the die width cause extensive motion of the stamp into the film without any additional normal load.

Figure 2 summarizes key features of SAOSF. High-resolution features are fully preserved by SAOSF despite the lateral motion of the die, as demonstrated in panels a–d in Figure 2. Lines of 60 nm are inscribed by focused ion beam (FIB) milling on a circular punch face (Figure 2a,b). Their imprint is barely visible at 90 MPa normal loading (Figure 2c), but they are very well replicated during subsequent shear forming (Figure 2d). SAOSF is capable of driving more complex flows—the filling of 225 nm half-pitch, deep grooves present on the stamp of Figure 2f can be significantly enhanced by the shear process (Figure 2h), beyond the normal loading (20 mN) shown in Figure 2g. This parallel shear flow was realized over an area of 15 μm in diameter also with 20 mN normal load applied. Very large long-range mass movements are achievable while maintaining these nanoscopic features and their registry. In Figure 2e, shear forming at 350 MPa normal pressure was sufficient to reduce the residual layer reachable by normal loading alone by a factor of 4, from 350 nm to about 90 nm. That is an aspect ratio increase from about 7 to 30. This filling could be achieved by motion of the die both normal to and parallel to the lines. In general, nanoscopic features are readily formed, while mass transport over larger distances remains the main challenge in nanoimprint. We are currently limited in achieving further increases in patterned area by the lateral compliance of the indentation system.

An example of displacements throughout a single imprint and shear forming process is shown in Figure 3a. Initial normal loading produces indentation into the film. Subsequent shear motion, first started with mean amplitude 2.0 nm, has no effect on the stamp normal displacement until its amplitude is increased to a threshold of about 4 nm. A minimum shear strain of the film is thus required to initiate shear forming; for glassy polymers, we find this to be typically 0.5% and largely independent of the die diameter. Beyond this threshold shear strain, the stamp resumes its normal motion into the sample, increasingly so as the shear amplitude is further increased.

Material transport in SAOSF scales with both shear amplitude and number of cycles as seen in the experimentally measured extrusion map of Figure 3b. At mean normal pressure of 440 MPa, the threshold amplitude for shear forming activation (shown explicitly in Figure 3a) is visible, with large cycle numbers having little effect below about 5 nm. Beyond the threshold amplitude, extrusion scales with the number of cycles. It is also initially proportional to the product of the number of oscillation cycles and the shear amplitude, implying a cumulative effect of plastic deformation

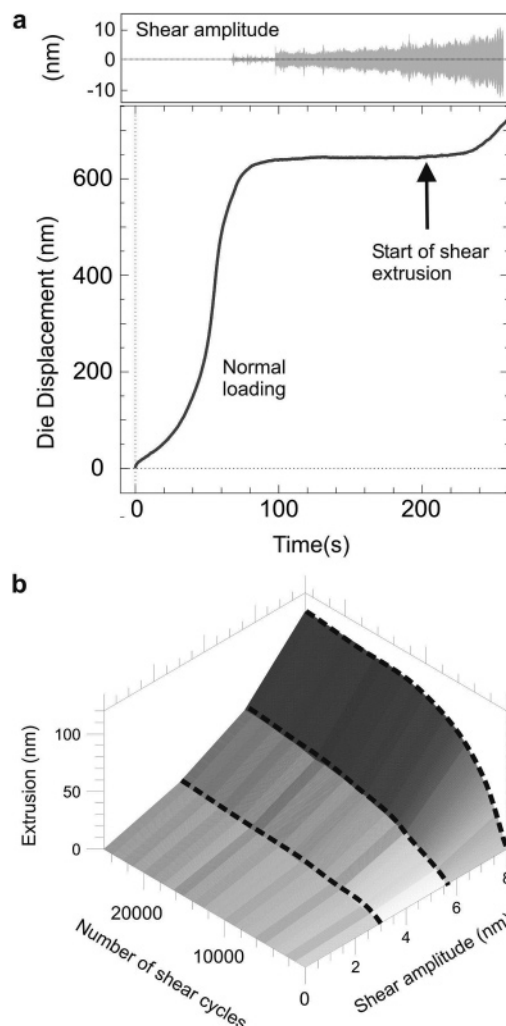


Figure 3. Threshold amplitude and cycle number dependence for shear-based solid forging. (a) The displacement of a forming die into a 950 nm thick polystyrene film is measured against time as it is loaded to a pressure of 440 MPa and depth of 650 nm. Shear action is then applied with the measured amplitude envelope (top). Extrusion of the film resumes once a shear amplitude threshold of about 4 nm is reached. (b) The general behavior of shear-induced extrusion with amplitude and number of cycles. Below the threshold amplitude of about 4 nm there is little enhancement of extrusion. Above the threshold, the extrusion increases with amplitude and number of cycles but eventually reaches a limiting depth in all cases. The dashed lines indicated the actual data taken.

tion from each cycle on overall mass transport. We point out that this means the film thickness can be deliberately controlled by choosing the number of cycles. The relation to number of cycles at fixed amplitude is lost at high cycle numbers. This is partly because as the film thins, its lateral stiffness increases, so more of the applied shear displacement is taken up by the (fixed) shear stiffness of the die itself rather than the film. That is, the effective drive amplitude decreases. For extremely thin layers, nonuniformity of the die–substrate separation may matter.

To elucidate the detailed mechanism of SAOSF, we have performed finite element analysis (FEA) of a simple, ductile J_2 -yield system under indentation plane strain (see Supporting Information for further details.) First we note that the shear strain required to initiate SAOSF plasticity does not scale

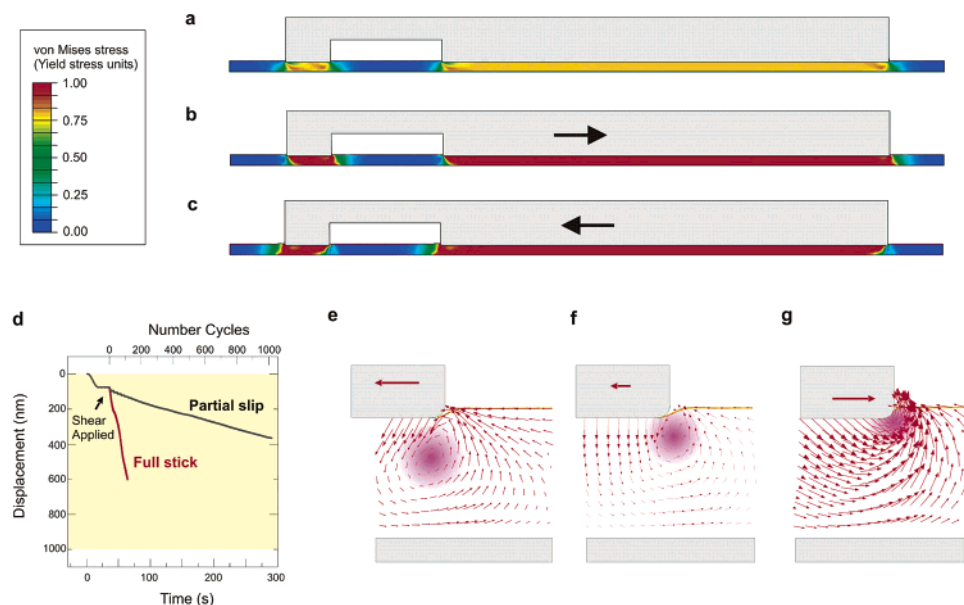


Figure 4. Mechanism of SAOSF. (a) Contours of von Mises stress calculated by plane strain finite element analysis (FEA) indicate only an elastic response produced in a generic elastic–elastoplastic film at modest normal load, while a complete state of plasticity (red contour) under small and large stamp features is easily developed when a 7% shear strain is imposed in either the right or left directions (b and c) at the same normal load. That the technique is insensitive to die–sample boundary conditions is demonstrated in (d), where a change from full stick to partial slip friction conditions effect only the per-cycle rate of shear extrusion. The second essential component of shear extrusion for solids is given by circulation at Cauchy points of the die tooth. The material displacement vector field at the right-hand corner of a stamp tooth is shown for left stroke (tensile) through right stroke (compressive) shear loading of the contact in parts e–g. A region of material circulation (purple) moves up from slightly below the surface in part e to “break” against the stamp sidewall in part g. For each cycle, the broken symmetry of this circulation results in a net pumping of material from beneath the tooth to the adjacent free-surface regions.

with die diameter at all. Critically, this means that a wide variety of feature sizes and scales can be simultaneously shear formed in the planar geometry. The plot of Figure 4a provides contours of von Mises stress at low normal indentation load of a two tooth die, where the Cauchy stress singularity points at the corners of the teeth create small highly localized regions of material in a plastic state. Introducing a small shear displacement 7% of the film thickness, we see that a plastic state (red contour) is introduced across the whole of both the narrow and wide teeth of the punch, in both shear stroke directions (parts b and c of Figure 4). Oscillating this shear in the simulation, we find that we are readily able to reproduce the full SAOSF extrusion effect (see Supporting Information for movies.)

In conventional forming operations where high aspect ratio geometries present large, compressive contact areas, friction between die and billet leads to an exponentially rising “friction hill” and mean forming stress.¹⁵ Lubricating interfacial layers provided by injecting liquid or by ultrasonic interfacial melting¹⁶ attempt to mitigate this frictional effect. In Figure 4d we show that our technique is *not* due to modification of boundary conditions or lubrication. In fact, the opposite is found in SAOSF—full stick boundary conditions produce the strongest effect per cycle. We can induce SAOSF under a wide range of slip to no-slip conditions, with some minimal normal loading requirements. The SAOSF action is thus more akin to pumping. It relies on amplifying a small transport hysteresis by repetition.

The material motion can be visualized by the nodal motion of the finite element mesh (Figure 4e–g, also see displace-

ment movie, Supporting Information). A circular flow pattern occurs about each Cauchy point (corner edge) of the stamp, synchronized to the shear oscillation. The symmetry of this circulation is broken by the vertical punch side wall, causing a gradual migration of material to the pile-up region at the stamp sides. This is especially evident on the compressive side of the shear stroke shown in Figure 4g, where large vertical displacement vectors at the stamp edge reflect motion of material into a forming chip. SAOSF thus relies on structural ratcheting arising from contact induced, nonuniform stress distributions⁴ and will operate regardless of any material ratcheting that may also accompany and enhance it.¹⁷

When operated at low frequencies (0.1 Hz), SAOSF shows incremental normal stamp motion on each cycle with high vertical displacement rate correlated to the maximum shear rate and going to zero with each turning point in the oscillatory shear motion (see Supporting Information.) This behavior is mirrored in the isothermal simulations. Postimprint inspection of dies by scanning electron microscopy shows no significant material transfer, nor do we measure any increase in adhesive pull-off force over a broad range of forming frequencies. While a direct measurement of the thin film temperature remains to be performed, the above arguments provide strong evidence that the SAOSF process occurs with no significant temperature rise. This is further supported by a spreading resistance calculation (Supporting Information) showing that for shear amplitudes up to 10's of nanometers and frequencies in the kilohertz regime, the expected temperature rise remains well below 1°. The per-

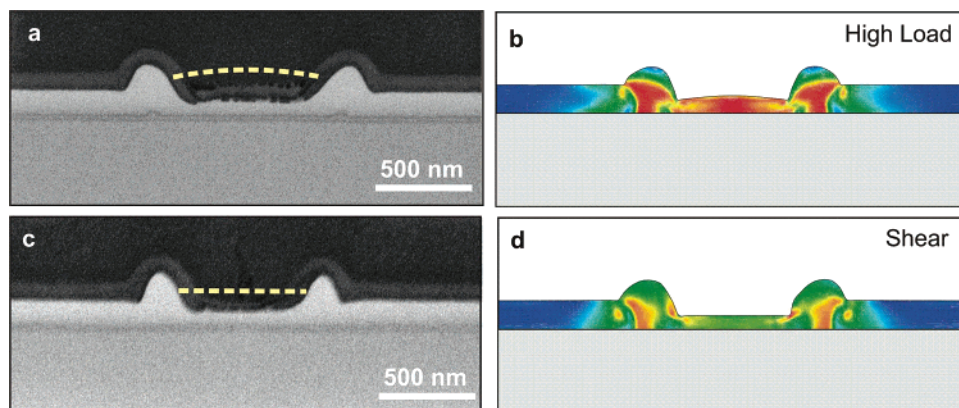


Figure 5. Critical forming defects are avoided by shear forming. Attempts to thin a film by simply applying high pressure lead to loss of residual layer uniformity, experiment at 1 GPa in a and simulation in b, while employing the SAOSF technique under a low normal pressure (150 MPa) produces a flat residual layer, c and d. This can be understood by the significantly lower degree of residual stress (partially shown here by von Mises stress contours, scale equivalent to that of Figure 4) left by the shear process as indicated by the simulations b vs d. Continued shear action thinning of the residual layer while retaining uniformity is easily achieved as shown in Figure 2h. Scanning electron micrographs of FIB-milled cross sections in (a, b) show polymer in bright white, with a 150 nm gray halo due to a deposited platinum masking layer.

cycle nature of shear forming means that fidelity vs throughput tradeoffs present in normal loading schemes¹³ can be overcome by increasing the oscillation frequency. We find that at very high frequencies (~ 100 's kHz) the system does heat up, as indicated by thermal expansion driven reverse motion of the stamp which is easily detected by the sensitive displacement measurement capability of the nanoindenter. This gives the known problems upon subsequent cooling.¹² At typical low kilohertz frequencies, however, the process appears isothermal. Since at most a few hundred cycles are usually required for the pumping action, the overall process is rapid.

Figure 5 illustrates a key fidelity difference between simple normal loading and SAOSF. Plane strain experiments using a 600 nm by 6000 nm rectangular punch on a 150 nm polystyrene film show excellent qualitative feature matching to geometrically congruent, partial-slip finite element simulations. Attempts to thin the film by simply applying high load (~ 1.0 GPa) show how instead, for both experiment (a) and simulation (b), a loss of residual layer uniformity occurs. In ref 8 this was shown to be due to elastic deformation of the die. In contrast, shear forming using a far lower normal load (150 MPa) leads to an excellent uniformity for the same degree of thinning, (c) and (d). This uniformity is of crucial importance, for instance, to critical dimension (CD) yields produced during further processing steps in lithographic applications^{10,13,18,19} and to gate electrode operation via uniform and thin insulating layers in field effect transistors. Shear forming therefore provides a way to overcome the limitations of die elastic deformation. These are more significant for large areas, since normal force scales with area, but die rigidity scales with diameter for features on a solid hinterland.⁸ Nanoscale features of a dimension smaller or equivalent to the film thickness are by comparison relatively straightforward to form—it is multiscale flow arising from an initial distribution of feature sizes and a cascade of progressively filled regions that provides the challenge.

In summary, we have demonstrated a new solid processing technique under constant room temperature conditions for simple die shapes in thin, glassy polymer films. Finite element simulation agrees well with experiment and suggests that the process is due to combination of uniformly plasticizing the whole film, and a novel pumping action involving die-geometry-induced broken circulation of elastoplastic flow. It is an isothermal process, free of temperature ramping times, thermal stresses, and adhesion problems during die removal, with material deformation localized to regions very close to the die. Nanometer dimension feature fidelity is preserved under its operation, and it appears readily scalable from nanoscopic to 10's of micrometer dimensions. Crucially, the process is scale independent for thin film planar forming, since a critical shear *strain* is required. Reduced normal forging load largely eliminates elastic distortions, and the process appears relatively insensitive to die–film friction. The potential of SAOSF to activate transport in a wide choice of solid imprint materials may eventually extend to self-assembled nanomaterials amenable to plastic flow, furnishing a connection between “top-down” and “bottom-up” patterning techniques.

Acknowledgment. This work was made possible by funding support from Science Foundation Ireland under Grant 00/PI.1/CO28.

Supporting Information Available: Extended description of the experimental and modeling methods and mechanical simulation movies are provided. This material is available free of charge via the Internet at <http://pubs.acs.org>.

References

- (1) Chou, S. Y.; Krauss, P. R.; Renstrom, P. J., Imprint lithography with 25-nanometer resolution *Science* **1996**, 272, 85–87.
- (2) Stutzmann, N.; Tervoort, T. A.; Bastiaansen, K.; Smith, P., Patterning of polymer-supported metal films by microcutting. *Nature* **2000**, 407 (6804), 613–616.
- (3) Khang, D. Y.; Yoon, H.; Lee, H. H., Room-temperature imprint lithography. *Adv. Mater.* **2001**, 13 (10), 749–752.

- (4) Colburn, M.; Johnson, S.; Stewart, M.; Damle, S.; Bailey, T. C.; Choi, B.; Wedlake, M.; Michaelson, T.; Sreenivasan, S. V.; Ekerdt, J.; Willson, C. G. *Proc. SPIE—Int. Soc. Opt. Eng.* **1999**, 3676, 379.
- (5) Xia, Y.; Kim, E.; Zhao, X.-M.; Rogers, J. A.; Prentiss, M.; Whitesides, G. M., Complex Optical Surfaces Formed by Replica Molding Against Elastomeric Masters. *Science* **1996**, 273, 347–349.
- (6) Stutzmann, N.; Friend, R. H.; Sirringhaus, H., Self-aligned, vertical-channel, polymer field-effect transistors. *Science* **2003**, 299 (5614), 1881–1884.
- (7) Guo, L. J., Recent progress in nanoimprint technology and its applications. *J. Phys. D: Appl. Phys.* **2004**, 37 (11), R123–R141.
- (8) Cross, G. L. W.; O'Connell, B. S.; Pethica, J. B., Influence of elastic strains on the mask ratio in glassy polymer nanoimprint. *Appl. Phys. Lett.* **2005**, 86 (8), 081902.
- (9) Johnson, K. L. *Contact mechanics*. Cambridge University Press: Cambridge, 1985.
- (10) Cross, G. L. W., The production of nanostructures by mechanical forming. *J. Phys. D: Appl. Phys.* **2006**, 39, R363–R386.
- (11) Ward, I. M.; Hadley, D. W. *An introduction to the mechanical properties of solid polymers*; John Wiley & Sons: Chichester, 1993.
- (12) Hirai, Y.; Yoshida, S.; Takagi, N., Defect analysis in thermal nanoimprint lithography. *J. Vac. Sci. Technol., B* **2003**, 21 (6), 2765–2770.
- (13) Schulz, H.; Wissen, M.; Bogdanski, N.; Scheer, H.-C.; Mattes, K.; Friedrich, C., Impact of molecular weight of polymers and shear rate effects for nanoimprint lithography. *Microelectron. Eng.* **2005**, 83, 259–280.
- (14) Cross, G. L. W.; O'Connell, B. S.; Langford, R. M.; Pethica, J. B., The mechanics of nanoimprint forming. *Mater. Res. Soc. Symp. Proc.* **2004**, 841, R1.6.
- (15) Dieter, G. E. *Mechanical metallurgy*; McGraw-Hill: London, 1988.
- (16) Eaves, A. E.; Smith, A. W.; Waterhouse, W. J.; Sansome, D. H., Review of the application of ultrasonic vibrations to deforming metals. *Ultrasonics* **1975**, 162.
- (17) Hübel, H., Basic conditions for material and structural ratcheting. *Nucl. Eng. Des.* **1996**, 162, 55–65.
- (18) Hong, P. S.; Lee, H. H., Pattern uniformity control in room-temperature imprint lithography. *Appl. Phys. Lett.* **2003**, 83 (12), 2441–2443.
- (19) Gourgon, C.; Perret, C.; Micouin, G.; Lazzarino, F.; Tortai, J. H.; Joubert, O.; Grolier, J.-P. E., Influence of pattern density in nanoimprint lithography. *J. Vac. Sci. Technol., B* **2003**, 21, 98–105.

NL0624566